The DTU21 Global Mean Sea Surface and First Evaluation

Ole Baltazar Andersen[1], S. K. Rose[1], A. Abulaitijiang[2], S. Zhang[3], S. Fleury[4]

[1]DTU space, National Space Institute, Elektrovej 327/328, DK-2800 Kongens Lyngby, Denmark.

[2]University of Bonn, Institute of Geodesy and Geoinformation Nussallee 17, D-53115 Bonn, Germany

[3]School of Resources and Civil Engineering, Northeastern University, Shenyang, China

[4]LEGOS, Observatoire Midi-Pyrénées 14, avenue Édouard Belin 31400, Toulouse, France

*** Correspondence:**
Ole Baltazar Andersen
oa@space.dtu.dk

Keywords: altimetry, mean sea surface, retracking, geodetic mission, long repeat orbit.

Abstract

A new Mean Sea Surface (MSS) called DTU21MSS for referencing sea level anomalies from satellite altimetry is introduced in this paper and a suite of evaluations are performed. One of the reasons for releasing an updated Mean Sea Surface is the fact, that during the last 6 years nearly three times as many data have been made available by the space agencies, resulting in more than 15 years of altimetry from Long Repeat Orbits or Geodetic Missions. This includes the two interleaved long repeat cycles of Jason-2 with a systematic cross-track distance as low as 4 km.

A new processing chain with updated filtering and editing has been implemented for DTU21MSS. This way, the DTU21MSS has been computed from 2Hz altimetry in contrast to the DTU15MSS which was computed from 1 Hz altimetry. The new DTU21MSS is computed over the same 20-year averaging time from 1993.01.01 to 2012.12.31 with a center time of 2003.01.01.

Cryosat-2 employs SAR and SARin modes in large part of the Arctic Ocean due to the presence of sea ice. For SAR and SARin mode data we applied the SAMOSA+ physical retracking (Dinardo et al., 2018) in order to make it compatible with the physical retracker used for conventional Low Resolution Mode data in other parts of the ocean.

1 Introduction

Satellite altimetry provides highly accurate measurement of the ocean topography along the ground tracks of the satellite (Fu and Cazenave, 2001; Stammer and Cazenave, 2019). For oceanography, the anomalous sea level about a mean reference surface is of primary interest. During the last two decades, Mean Sea surface as a reference surface has been developed with increasing accuracy (Pujol et al., 2018). Sea level observations contain information on all timescales.

To develop a Mean Sea Surface (MSS) it would be optimal if observations were available on all time and spatial scales. The challenge is to derive an MSS given limited sampling in both time and space using satellite observations. Another challenge is to merge repeated observations along coarse ground tracks with high spatial data from the geodetic mission (GM).

Thanks to new altimeter instruments and processing technology the accuracy of Sea Surface Height (SSH) have increased dramatically over the last decade. It is important for deriving the Sea Level Anomalies (SLA), that the reference or MSS is as accurate as the SSH in order to investigate smaller mesoscale features (e.g., Dufau et al., 2016).

The paper is structured in the following way. Chapter 2 presents the details of the derivation of the new DTU21MSS with focus on the improvement in data, retracking, processing and filtering. The chapter is concluded with a subsection on the potential use of Sentinel-3A for the DTU21MSS. Chapter 3 highlights various initial comparison ranging from an initial global comparison to Arctic and coastal comparisons to illustrate the various improvement in the MSS models.

2 Computation of the DTU21MSS

The DTU21MSS is based on satellite altimetry data from frequently repeating Exact Repeat Missions (ERM) and in-frequently repeating missions with long repeat – called Geodetic Mission (GM). The MSS is determined from a sophisticated combination of the coarse ERM with the high-density GM data as described in Andersen and Knudsen (2008).
The first step is to select the averaging period and consequently the center time for the MSS. For all available DTU MSS models MSS is computed over the 1993.01.01 to 2012.12.31. Hence the center time for all DTU models will be 2003.01.01. Within the 66º parallels the highly accurate mean profiles derived using TOPEX/J1/J2 nearly uninterrupted observations is the back-bone of the MSS models.
Table 1 shows all altimetry used for the computation of the DTU21MSS and its predecessors: DTU15MSS and DTU18MSS. Whereas the DTU15MSS was based on roughly 5 years of GM observations, the DTU21MSS is based on nearly three times as much data or more than 15 years of GM due to the recent focus on launching satellites in long repeat orbits.

It is also important that satellite observations from the four newer GMs (Cryosat-2, Jason-1, Jason-2 & SARAL) have around 1.5 times higher range precision compared with the old ERS-1 GM (Garcia et al., 2014) Consequently it was decided to retire the ERS1 GM data for the DTU21MSS due to its inferior signal to noise ratio.

	Satellite	DTU15MSS	DTU18MSS	DTU21MSS
ERM	TP+Jason-1+Jason-2	Jan 1993- Dec 2012	Jan 1993- Dec 2012	Jan 1993-Dec 2012
	ERS2+ENVISAT	May 1996-Oct 2011	May 1996-Oct 2011	May 1996-Oct 2011
	TP & Jason-1 Interleaved	Sep 2002 to Oct 2005 Feb 2009 to Mar 2012	Sep 2002 to Oct 2005 Feb 2009 to Mar 2012	Sep 2002 to Oct 2005 Feb 2009 to Mar 2012
	GFO	Jan 2001 Aug 2008	Jan 2001 Aug 2008	Jan 2001 Aug 2008
GM	ERS1 (2 interleaved cycles of 168 days)	April 1994-May 1995	April 1994-May 1995	Not Used
	Cryosat-2 (368.25 days repeat	Oct 2010-July 2014	Oct 2010-July 2017	Oct 2010- Oct 2019
	Jason1 LRO (1 cycle of 404 days)	April 2012-Jun 2013	April 2012-Jun 2013	April 2012-Jun 2013
	Jason2 LRO (2 cycles of 371 days)	Not used	Not used	Aug 2017-Sept 2019
	Saral AltiKa (drifting phase)	Not used	Not used	July 2016-Dec 2020

Table 1. Satellite altimetry used for the DTU15/18/21MSS models.

The DTU21MSS builds on a slightly filtered version of the DTU15MSS. There have been major theoretical advances leading up to the release of the DTU21MSS compared with the previous

DTU15MSS. After describing the altimetric data in the next section, these are detailed in the subsequent sub-sections below. One advance is related to the retracking and range precision of the data. Another advance is related to the computation of new 2-Hz altimetric observations. The final advance is related to long wavelength corrections and the use of anisotropic filtering to enhance the MSS in current regions and Polar regions.

2.1 Satellite altimetry

The Sensor Geophysical Data Record (SGDR) products for Jason-1 GM, Jason-2 GM, and SARAL/AltiKa GM are obtained from the Archiving, Validation, and Interpretation of Satellite Oceanographic (AVISO) data service. The L1b-level products for CryoSat-2 LRM are acquired through the data distribution service of the European Space Agency (ESA). All these products include along-track high- sampling-rate waveforms equivalent to 20 Hz for all missions except for 40 Hz for SARAL/AltiKa.
All environmental and geophysical corrections of the altimeter range measurements have been applied to calculating Sea Surface Heights (SSH). These corrections include dry and wet tropospheric path delay, ionospheric correction, ocean tide, solid earth tide, pole tide, high-frequency wind effect, and inverted barometer correction. The most recent FES2014 ocean tide model has been used for all missions (Lyard et al., 2021). All corrections are provided on 1-Hz. Hence, these were interpolated into 20 Hz or 40 Hz by using piecewise cubic spline interpolation.
All satellites except for CryoSat-2 operate in the traditional low-resolution mode (LRM) where the along-track resolution is limited to 2-3 km. Cryosat-2 also operates in LRM over most of the oceans. In regions where sea ice is prevailing Synthetic Aperture Radar (SAR) is applied. In this mode, the returning echoes are processed coherently resulting in a footprint of 290 meters. Over steeply varying terrain and in some coastal regions, the SAR interferometric mode (SARin) is used where the instrument receives on two antennas are used. A mode mask controls the availability of three data types (www1, 2022). The advantage of the SAR processing is in theory a factor of 2 improvements in range precision (Raney., 2011). Due to the burst structures of Cryosat-2, the improvement found is only around 1.5 times the range precision of LRM data. (Raney, 2011; Garcia et al., 2014)

Waveform retracking is an effective strategy to improve the range precision of altimeter echoes (Gommenginger et al., 2001). There are two strategies. Empirical retracker has the advantage of providing a valid and robust estimation of arrival time used for sea surface height (SSH) estimation for almost all types of surfaces (e.g., sea ice leads, coastal). The disadvantage is that they only provide SSH and not rise time used to determine significant wave height and windspeed important to derive a Sea State Bias correction (Fu and Cazenave, 2001).

Physical retrackers generally apply the Brown model for LRM data (Brown 1977) or the SAMOSA model for SAR and SAR-in observations (Ray et al. 2015). These estimate 3 or more parameters and enable corrections and sea state conditions, through the determination of significant wave height and wind speed.

2.2 Two-pass retracking for range precision

Over the ocean, the typical shapes of raw waveforms from all four GM satellite missions are well-modeled using the Brown-type model. In the first step, the waveforms are fitted by the three-parameter Brown model (arrival time, rise time, and amplitude).

However, (*Maus et al.,* 1998; *Sandwell and Smith,* 2005) showed that there is a strong coherence between the estimation errors in the arrival time and rise time parameters resulting in a relatively noisy estimate of arrival time and hence sea surface height. Consequently, Sandwell and Smith (2005) suggested the use of a second step where the rise time parameter is smoothed. In the derivation of the DTU21MSS, we applied the same two-step retracking and fixed the along-track smoothing at 40 km before retracking the waveforms again using a two-parameter Brown model (arrival time and amplitude).

For the four GM missions Jason-1, Jason-2, SARAL/AltiKa, and CryoSat-2/LRM this approach has been proved effective (Garcia et al. 2014; Zhang and Sandwell 2017). Figure 1 illustrates the gain in range precision using the two-pass retracking. The improvement for all four LRM datasets is dependent on the SWH but is on average of the order of 1.5 similarly to what has been shown by other authors. (Sandwell et al,, 2014; Zhang et al., 2019).

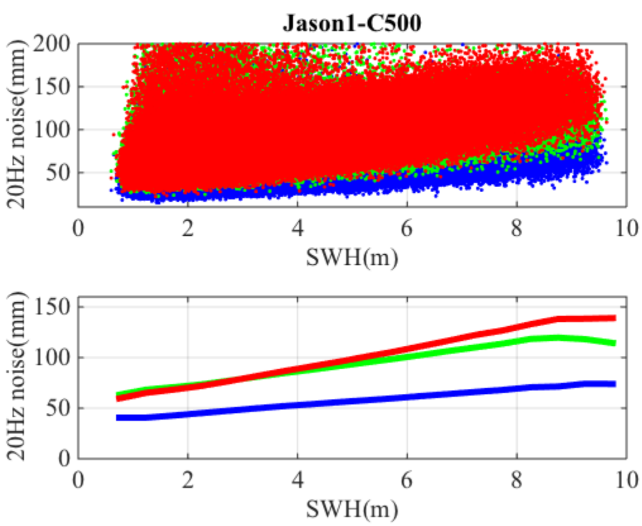

Figure 1. The standard deviation of retracked height with respect to DTU15MSS for the first 11 days of the Jason-1 GM. The upper figures illustrate the statistics for individual points. The lower figure illustrates the median averaged over 0.5 meters SWH intervals. Red: height from sensor geophysical data record; Green: height from the first step of two-pass retracking; Blue: height from the second step of the two-pass retracking). Modified from Andersen et al., (2021)

Commented [AA1]: It seems the figure shows the cycle 500 of Jason-1 GM. So if it is only one cycle for Jason-1 GM, it is roughly 11 days.

Whereas two-pass retracking is very efficient for LRM data, we did not apply the two-pass retracking for the CryoSat-2 SAR- and SARIN-mode data as there is no gain in range precision from the second step of the retracking. This was documented by Garcia et al., (2014).

2.3 2-Hz Sea Surface height data

The 20/40Hz double retracked SSH data are edited for outliers and subsequently, an along-track low-pass filtered is applied before generating the 2Hz SSH data used for MSSH determination.

The along-track low pass filter uses the Parks-McClellan algorithm which has a cut that begins at 10 km wavelength and zero gain at 5 km, thus has 0.5 gain at 6.7 km, which is approximately the resolution of 1Hz data. (Sandwell and Smith, 2009). The filter had to be designed for each satellite mission to match the 0.5 gain at 6.7 km due to the different along-track sampling rates. After this filter is applied the data were downsampled to a 2 Hz sampling rate, which corresponds to an along-track spacing of around 3 km.

For the previous DTU15MSS we used 1 Hz or roughly 6 km along track SSH data from the Radar Altimetry Data Archive (RADS, Scharroo et al., 2013). The 1 Hz data have been generated using a boxcar filter or the equivalent of computing the 1 sec mean of the available 20/40Hz data. The advantage of using of the Parks-McClellan algorithm over the boxcar filter is that this filter does not introduce side lobes degrading the SSH in the 10-40 km band contributing to the spectral hump of conventional LRM data (Dibarboure et al., 2014; Garcia et al., 2014). This is illustrated in Figure 2.

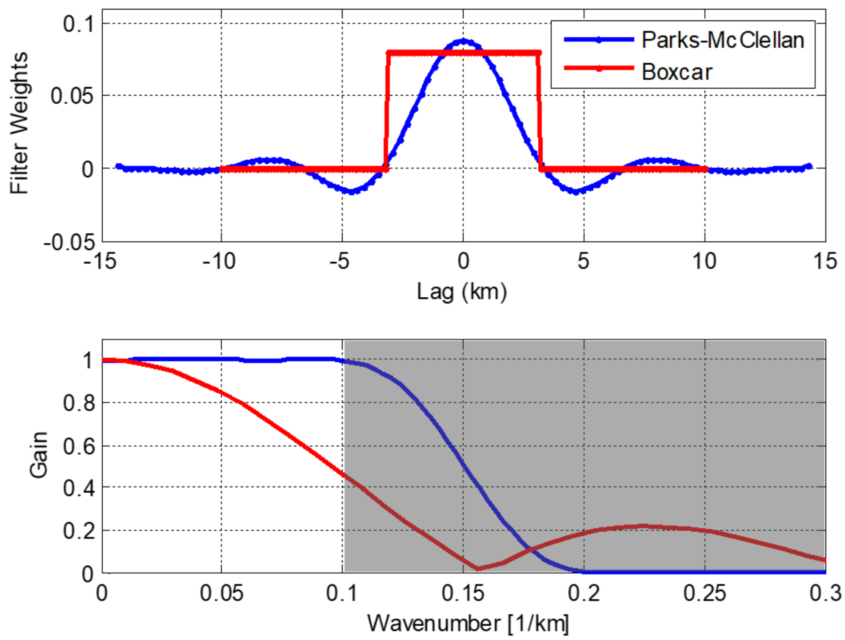

Figure 2. Illustration of Parks-McClellan filter used to derive consistent and stable 2Hz Sea surface height.(top) spatial filter function of boxcar (in red) and Parks-McClellan filter (in blue) (bottom) frequency response of the two filters. Sidelobes and spectral leakage at the short wavelengths can be observed for the boxcar filter, which will remain as high-frequency noise in the filtered dataset.

2.4 Long-wavelength adjustment

The DTU21MSS builds on the heritage of the DTU15MSS. We first compute a long wavelength correction using the ERM mean profiles. This is done separately inside the 66 º parallel corresponding to mid and low latitude regions where the TOPEX/J1/J2 are available and outside the 66 º parallel where we have to rely on other satellites.

2.4.1 Mid and low latitudes

The long wavelength of the MSS within the 66º parallels largely defined by the highly accurate mean profiles derived using TOPEX/J1/J2 nearly uninterrupted observations every 9.91 days for 20 years. Along the mean profiles, the 2Hz mean profiles are computed every 3 km, but across tracks, the sampling is far less and up to 330km at the Equator.
The major ocean currents (e.g., the Gulf Stream and Kuroshio) flow largely west to the east giving rise to a significant MSS signal.

Compared with its predecessor DTU15MSS and DTU18MSS we improve the modeling of large currents using an an-isotropic covariance for the interpolation using least squares collocation. In the interpolation a second order Gauss-Markov covariance model with a correlation length of 300 km in the longitude direction and 100 km in the latitude direction. The result is a small correction in the major current systems which ranges up to 5 cm.

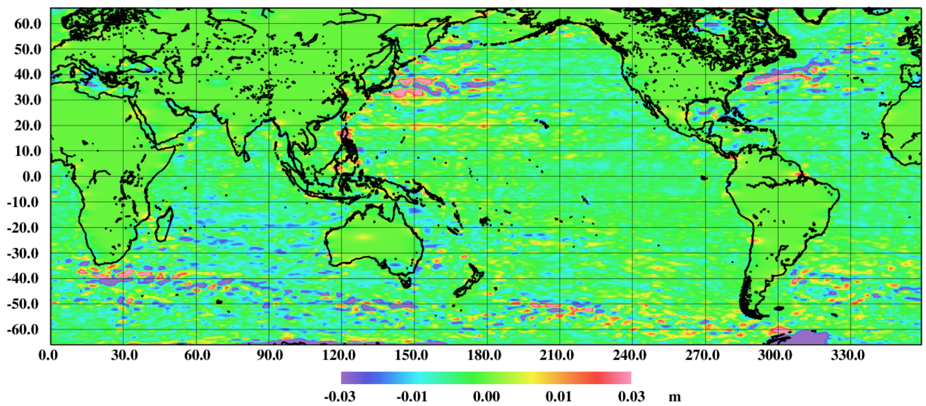

Figure 3. The long wavelength correction to DTU15MSS computed from the TOPEX/J1/J2 mean profiles inside the 66º parallel and from the ERS-2+ENVISAT mean tracks outside the 66º parallel.

2.4.2 Polar region MSS from Cryosat-2

A closer inspection of the Cryosat-2 mode mask (www1, 2022) shows that Polar Regions (outside the 66 º parallels) are largely measured in the SAR and SARin modes due to the presence of sea ice. This is with the exception of the Barents Sea north of Norway.
For SAR and SARin mode data we applied the SAMOSA+ physical retracking (Dinardo et al., 2018). SAMOSA+ adapts the SAMOSA retracking model (Ray et al., 2015) to operate over specular scattering surfaces as ice-covered polar oceans by involving mean square slope as an additional parameter in the retracking scheme and by implementing a more sophisticated choice of the fitting initialization resulting in greater robustness to strong off-nadir returns from land or else. The SAMOSA+ retracker even discriminates between return waveforms from diffusive and specular scattering surfaces, ensuring the continuity in the sea level retrieval going from the open ocean and into the sea, since it falls back to the standard SAMOSA solution over the open ocean.

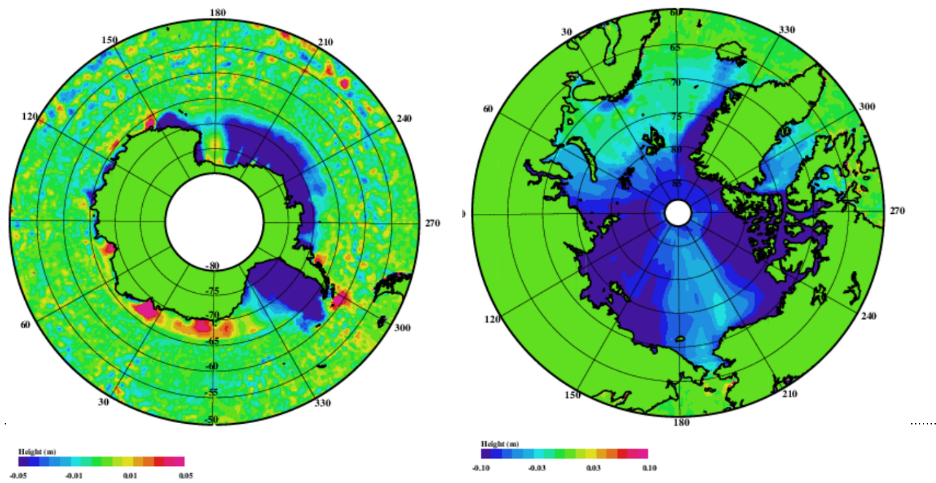

Figure 4. DTU21MSS-DTU15MSS for the Southern Ocean (left) and the Arctic Ocean (right). The color scale ranges up to +/- 5 cm for the Southern Ocean and +/-10cm for the Arctic Ocean.

With the assistance of the European Space Agency (ESA) Grid Processing On-Demand (GPOD) we have processed a total of 9 years of Cryosat-2 (2010.10 to 2019.10) for both the Arctic and Southern Ocean using SAMOSA+ retracker. Observations over the sea ice have been removed, only observations over leads (ocean surface between the ice floes) remain. This post-processing is similar to Rose et. al., (2019).

Upon computing the mean of all observations, the center time for the Crysat-2 data was 2015.04 so it was necessary to correct for sea level rise to consolidate these data on the 2003.01 center period of the DTU15MSS and DTU21MSS following the methodology by (Rio and Andersen 2009). This was performed in the 65 º - 66º border zone as the reprocessing of Cryosat-2 with SAMOSA+ is limited to outside the 65 º parallels.

The difference between the DTU21MSS-DTU15MSS is shown in Figure 4 for the Southern Ocean close to Antarctica (left) and the Arctic Ocean (right). For nearly all ice-covered regions the DTU15MSS is higher than the DTU21MSS. DTU15MSS was derived from 1-Hz RADS data which were very sparse in both time and space. RADS converts the SAR data to Pseudo LRM (Scharroo et al,, 2013) and performed physical retracking on these data using a modified Brown model. In RADS many more data were available during the ice-free summer month where the annual signal causes sea level to stand higher, so it is expected that DTU15MSS could be too high.

2.5 Mean sea surface computation

The details of the computation technique of the DTU21MSS follows the development of former DTU MSS models (Andersen and Knudsen, 2008) where the ERM tracks are first used to computed the wavelength part of the MSS. Hereafter the GM data are introduced to compute the fine-scale structures of the MSS. This part uses small tiles to parallelize the computation process.

The final step to close the Polar Gap is to fill in MSS proxy data north of 88N where no altimetry is available. This was done by feathering the EGM08 geoid (Pavlis et al., 2012) across the pole in the following way: The preliminary MSS was calculated up to 88°N using the satellite altimetry data alone. Subsequently, the difference between the MSS and the EGM08 geoid was computed longitude-wise in the 87N-88N region and a mean offset was estimated and removed. The residual grid was transformed into a regular grid in Polar stereographic projection enabling interpolation across the North Pole using a second order Gauss Markov covariance function with a correlation length of 400 km. This makes the DTU MSS models truly global.

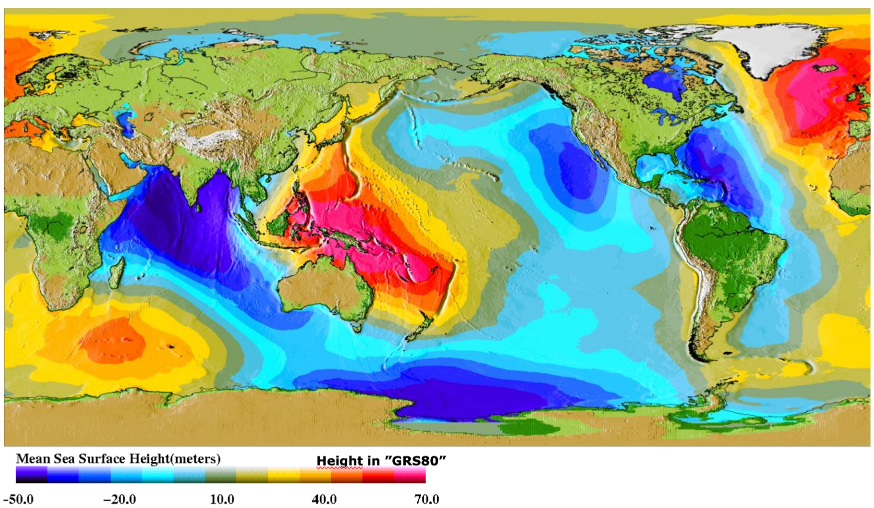

Figure 5. The mean sea surface from the Technical University of Denmark (DTU) in meters

The DTU21MSS as its predecessors is given on a 1-minute global resolution grid. A closer examination of the MSS in Figure 5 illustrates, that the height of the ocean's mean sea surface relative to the mathematical best fitting rotational symmetric reference system (GRS80) has magnitudes of 100 meters.

2.6 Sentinel-3

The European Space Agency (ESA) launched Sentinel-3A on the 16th of February 2016 and Sentinel-3B on 25th April 2018. These satellites operate as SAR altimeters everywhere with the benefit of increased range precision compared with conventional LRM altimetry. Both the increased along-track resolution and more importantly the cross-track resolution of 35 km would make these important contributors to the DTU21MSS. However, two problems prevented the use of these data for the time being.

The first relates to the fact that mean profiles could only be computed over 5 and 3 years from Sentinel 3A and B, respectively. As the Sentinel-3 satellites operate in a 27-days repeat this gave 66 and 40 cycles making these mean profiles considerably noisier compared with other mean profiles -

also because the satellites are sun-synchronous hence mapping S2 ocean tide residuals into the mean sea surface (Andersen and Knudsen, 2008). Secondly, the center times of the mean profiles are more than 15 years off the center time of the TOPEX/J1/J2 mean profiles. The effect of this is illustrated in Figure 6 showing a section of the Gulf Stream. Here the mean of S3A is 10 cm but the standard deviation of the Sentinel 3 mean profiles with respect to the DTU15MSS is 13 cm (Figure 6 left panel). The mean profile from Sentinel-3A along track 719 (blue arrow in the left panel) across the Gulf Stream is shown in the right panel going from south to north. Between 26N and 32N the difference corresponds closely to the expected sea level rise of a little more than 10 cm. However, as the track crosses the Gulf Stream the signal increases to nearly 60 cm.

The Gulf Stream causes the mean sea level to drop by around a meter as one moves from the south to north from the center of the Northwest Atlantic towards the coast. When the Gulf Stream meanders back and forth with time it creates the observed sea level residual seen (Zlotniki, 1991).

As Sentinel 3A and 3B are outside the (1993-2012) averaging period and as the meandering of the Gulf Stream is profound over the last 15 years, it was not possible to ingest the S3A and B mean profiles without degrading the DTU21MSS in this region.

There is no doubt to the importance of Sentinel 3A/B for future MSS models, but in order to ingest the Sentinel 3A/B in future MSS models we found, that we will need to extend the averaging period to 30 years (1993-2022).

We consequently decided to use the Sentinel 3A/B for the evaluation of the various MSS models.

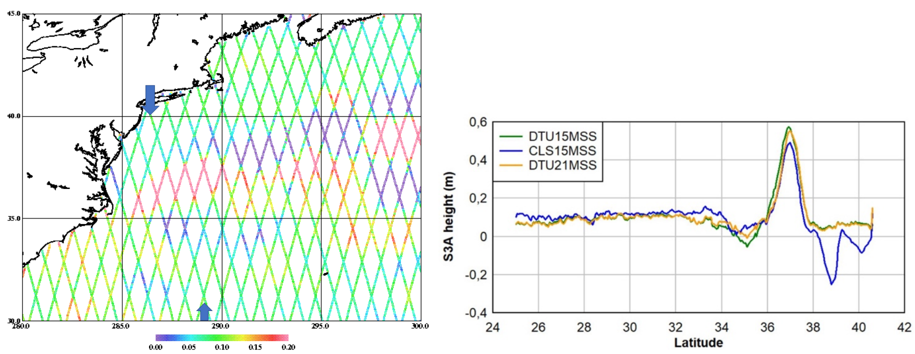

Figure 6. Sentinel-3A 5y mean profiles in the Gulf Stream area (left) relative to the DTU15MSS. The Sentinel-3A mean profile for track 471 (blue arrow) across the Gulf Stream relative to the DTU15MSS, the CLS15MSS (Schaeffer et al, 2012), and the DTU21MSS

3 Evaluation

In this section, we perform three different evaluations of the MSS. These evaluations are by no means as complete as the evaluation performed by Pujol et al. (2018) but serve the purpose of indicating the improvements going from DTU15MSS to DTU21MSS globally, in the Arctic Ocean, and in coastal regions.

3.1 Global evaluation with mean profiles

Most mean profiles have been used for the derivation of the MSS models. In the global comparison with mean profiles shown in Table 2, the TP/J1/J2, the TP/J1 interleaved, and the E2/ENV mean profile has been used in the deviation of all present MSS models. However, the S3A and S3B mean profiles are independent.

	TP/J1/J2 (541936)	TP+J1 Interleaved (542638)	E2/ENV (1652043)	S3A (1446733)	S3B (1418477)
DTU15MSS	0.00 /1.48	0.38 / 3.25	-0.17 / 3.97	4.92 / 5.20	4.94 / 5.39
DTU21MSS	0.00 / 1.17	0.36 / 3.21	-0.14 / 3.40	5.22 / 4.79	5.12 / 5.02
CLS15MSS	0.00 / 1.19	0.32 / 3.11	-0.17 / 5.22	5.26 / 5.01	5.01 / 5.18

Table 2. Comparison with mean profiles given as mean difference and standard deviation. All values are in cm. The (TP/J1/J2, TP/J1 interleaved and E2/ENV mean profiles, have been used in the deviation of the various MSS. The S3A/B mean profiles are independent.

Table 2 shows how the various models have been fit to the TP/J1/J2 mean profiles, which have both very small mean and standard deviation. In the comparison with the Sentinal-3A/B mean profiles, we limited the spatial extend to within the 65º parallels as the standard deviation increases considerably for the CLS15MSS at high latitudes. As has been demonstrated previously the oceans changes on all time scales and that, the more than 15 years of different time-epoch between the S3A/B mean profiles and the center epoch of the MSS models make the use of the S3A/B mean profiles unsuitable for the direct evaluation of the absolute accuracy of the MSS models. They do however indicate that the DTU21MSS performs superior compared with the older models from 2015.

3.2 Arctic evaluation.

Within the ESA CryoTempo project we evaluate the impact of the usage of a physical retracker and empirical retracker on the retrieval of sea level anomalies. We used the state-of-the-art empirical retracker called the Threshold First Maximum Retracker Algorithm (TFMRA) (Helm et al., 2014) and the SAMOSA+ physical retracker. In the evaluation, we also compared the state-of-the-art MSS models which were the DTU15MSS and DTU21MSS. It was not possible to compare with the CLS15MSS as this model only covers up to 84ºN and has several voids in the Arctic Ocean. The use of the physical retracker allows us to estimate the Sea State Bias (SSB) which was estimated. This Sea State Bias correction was subsequently applied to both the SAMOAS+ physical SLA and the empirical TFMRA SLA.
A total of 7 months of Cryosat-2 was used between Oct 3013 and April 2014. The results are shown in Figure 7 where the Upper panels show the spatial variation in the mean (two left panels for the empirical and physical SLA) and the corresponding standard deviation of SLA (two right panels). The lower panels highlight the time evolution of the monthly SLA anomalies averaged with the monthly mean given in the left panel and the standard deviation given in the right panel.

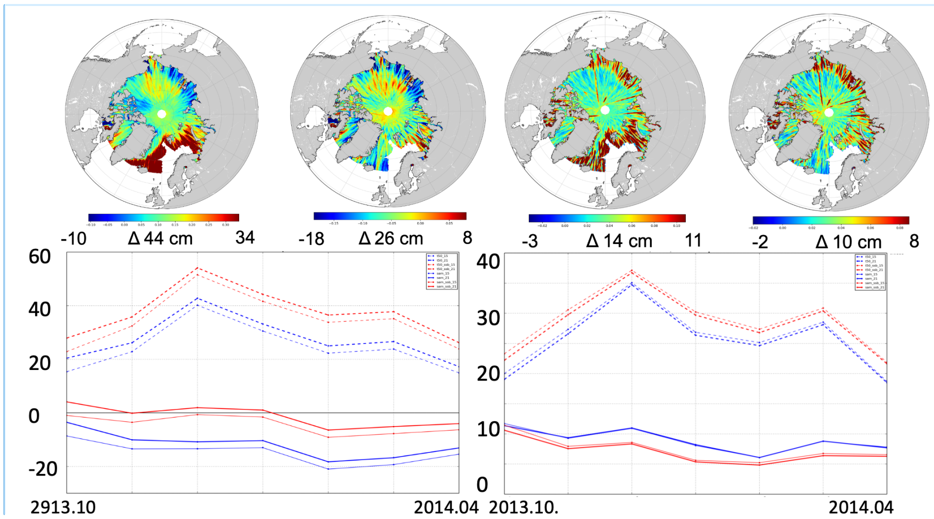

Figure 7. Comparison of retrackers and MSS models over the Arctic Ocean from Oct 3013-April 2014. Upper panels: Mean SLA using the empirical TMFRA retracker and DTU15MSS (first panel); Mean SLA using SAMOSA+ and DTU21MSS (second panel). Standard deviation of SLA using the empirical TMFRA retracker and DTU15MSS (third panel) and standard deviation of SLA using SAMOSA+ and DTU21MSS (fourth panel).
Lower panels: Evolution of SLA in time. Mean (left) and Standard deviation (right) shown as monthly values. Heavy lines correspond to using DTU21 and thin lines correspond to using DTU15. Dotted lines correspond to using the TFMRA retracker and solid lines to SAMOSA+ retracker. The red lines have the Sea State Bias correction applied whereas the blue lines have not.

This study shows an improved measurement of SLA using SAMOSA+. In conjunction with this physical retracker, the correction of the sea state bias (SSB) further improves the results. The SSB should not be applied with TFMRA50. In all cases, the DTU21MSS delivers better results than the DTU15 MSS. With SAMOSA+, SSB, and DTU21MSS we obtain a mean SLA of -1.5cm ±12cm instead of -5.4cm±22cm over the 2013/10-2014/04 period.

To illustrate the difference between various MSS models we computed the difference between the DTU21MSS and the DTU15MSS and CLS15MSS, respectively.

Commented [AA2]: Typo in the lower left edge of the figure. It should be "2013.10" instead of 2913.10.

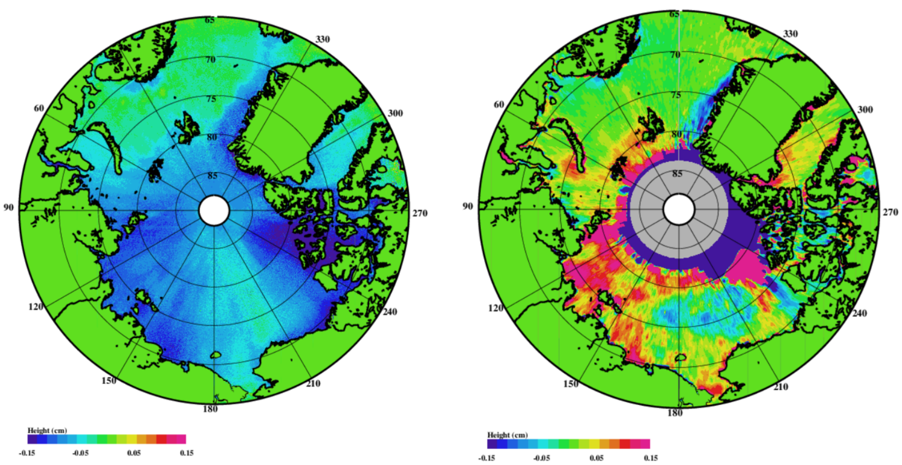

Figure 8 Difference (DTU21-DTU15) and DTU21-CLS15) for the Arctic Ocean. The color scale ranges from -15cm to +15 cm.

Figure 8 illustrates that the DTU21MSS is roughly 5-7 cm lower than the DTU15MSS throughout the Arctic Ocean. This is as mentioned previously an effect of the additional data for the DTU21MSS. Differences are small in the Northern Atlantic Ocean and the Barents Sea but increase to -14 -12 cm in the Canadian Arctic Archipelago.
The difference with the CLS15MSS highlight the fact that the MSS is limited to the 84ºN parallel. Also, the areas in blue north of Canada are voids in the CLS15MSS where the MSS values have been substituted by the EGM08 geoid.

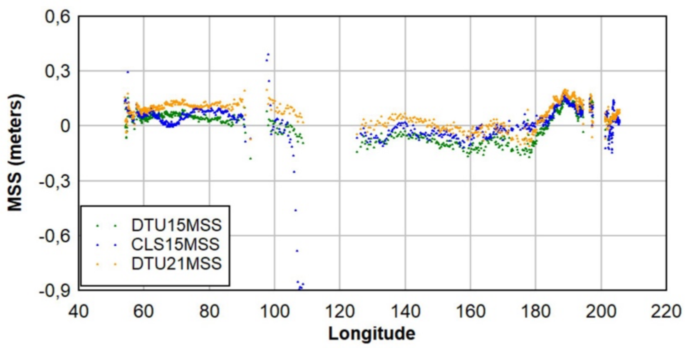

Figure 9. The difference between the 5-year S3A mean profile along track 497/498 and the various MSS models in the Arctic Ocean.

Another way of illustrating the differences between the various MSS model is to show the difference between a Sentinel-3A 5-year mean profile and the various MSS model. Figure 9 shows this difference along the Sentinel-3A track. The track transits from Russia at 68ºN,54ºE. Passing to the

east of Nova Zemlya and continues up to 82ºN (at 120ºE). From here it goes down to the Aleutian Trench at 57ºN, 204ºE. The standard deviation with the S3A mean profiles are 6.1 5.7 and 8.1 cm respectively for the DTU15MSS, DTU21MSS, and the CLS15MSS. The relatively large standard deviation of the CLS15MSS is related to large variations as close to sea ice as also indicated in Figure 8.
The increase in the S3A residuals around 190E is associated with the transition of the Bering Strait and the height on the eastern side of the Strait could be related to increased flow through the Strait (Woodgate and Peralta-Ferriz, 2021)

3.3 Coastal evaluation

The difference between the DTU21MSS and the DTU15MSS was evaluated in the Baltic Sea as part of the BalticSeal+ project (http://balticseal.eu/). Differences ranging up to 8 cm were found in the coastal zone and the narrow (15 km) Danish Straits as well as the Bay of Botnia and the Swedish archipelago. In all locations we found, that the former DTU15MSS is unreasonably high near the coastline. Similarly, we found that in the Bay of Finland the DTU15MSS was too low. In all cases, we found that this is an artifact of the gridding combined with the lack of 1Hz data used for the older DTU15MSS.

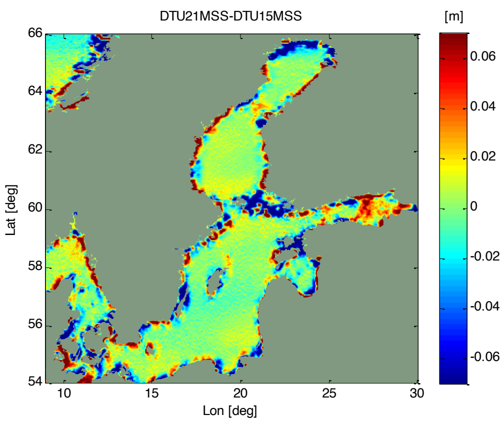

Figure 10. The difference between the DTU21MSS and the DTU15MSS in the Baltic Sea including the opening to the North Sea through the Danish Straits.

We investigated 5-year mean profiles from Sentinel-3A close to the Aleutian Islands in the northern Pacific Ocean. This is a major subduction zone and is well known for its huge gravity and geoid signal. Here we compared the various state-of-the-art mean sea surfaces DTU15MSS, CLS15MSS, and DTU21MSS. This comparison is presented in Figure 11. The difference between 5-year mean profiles from S3A and the various MSS are plotted along track 497.

We expect to find, that the S3A mean profiles would be around 5 cm higher due to a global linear sea level rise of 3 mm/year time over the 15 years due to the offset in the center periods of the MSS and the Sentinal-3A mean profile. The roughly 5 cm offset was confirmed by DTU15MSS and

DTU21MSS. The differences between the two indicate that DTU21MSS is generally only a few cm corrections to DTU15MSS. However, the difference with CLS15MSS shows some interesting oscillating effect of 15 cm up to 300 km from the coast in the CLS15MSS approaching the coast between latitudes 53.5 º and 56.5º. This is potentially some geoid residuals as CLS used a remove/restore technique with the EGM08 geoid model (Shaeffer et al., 2012). The same coastal oscillation was seen in most tracks in the region and also close to the coast in the NW Atlantic at track 471 shown in Figure 7.

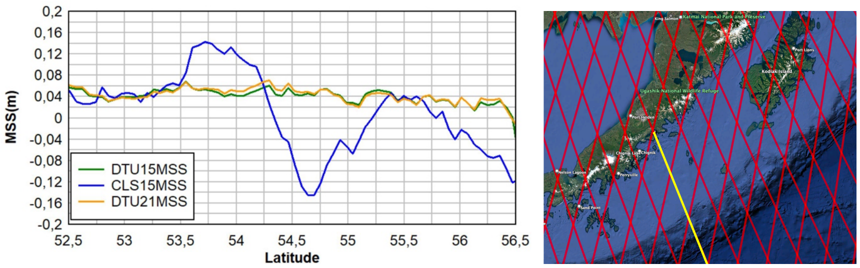

Figure 11. Difference between 5-year mean profiles from S3A along track 497. DTU15MSS (green), CLS15MSS (blue) and the DTU21MSS (green).

4 Conclusions

A new Mean Sea Surface (MSS) called DTU21MSS for referencing sea level anomalies from satellite altimetry has been presented along with the first evaluations. We have presented the updated processing chain with updated editing and data filtering. The updated filtering implies, that the 20Hz sea surface height data are filtered using the Parks-McClellan filter to derive 2 Hz. This has a clear advantage over the 1 Hz boxcar filter used previously in enhancing the MSS in the 10-40 km wavelength band. Similarly, the use of a the FES2014 ocean tide model improves the usage of sun-synchronous satellites in high latitudes in the new MSS.

Cryosat-2 employs SAR and SARin modes in large part of the Arctic Ocean due to the presence of sea ice. For SAR and SARin mode data we applied the SAMOSA+ physical retracking (Dinardo et al., 2018) in order to make it compatible with the physical retracker used for conventional Low Resolution Mode data.

We initially performed global comparisons with the mean profile from various available satellite using data from the RADS data archive as these have only been used in the DTU15MSS and not any of the other MSS models. Hence the comparison with these mean profiles can be slightly biased. However, the comparison with the 5- and 3-year S3A and S3B mean profiles are independent. These both shown a relatively clear improvement for the DTU21MSS which is also expected as the S3A/B data are derived from SAR altimetry and hence should compare better with the MSS derived using the two-pass altimetry due to the enhanced modelling of the 10-30 km wavelength (Garcia et al., 2013).

This the Arctic Ocean an initial study shows an improved measurement of SLA using SAMOSA+ with the DTU21MSS. In conjunction with this physical retracker, the correction of the sea state bias

(SSB) further improves the results. In all evaluations, the DTU21MSS delivers better results than the DTU15 MSS. With SAMOSA+, SSB, and DTU21MSS we obtain a mean SLA of -1.5cm ±12cm instead of -5.4cm±22cm over the 2013/10-2014/04 period.

Coastal evaluation of the new DTU21MSS was performed in the Baltic Sea and the Aleutian trench zone in Alaska. The evaluation in the Baltic Sea confirms that DTU15MSS is frequenlty several cm too high is coastal and Archipelago regions due to the lack of 1 Hz data for the DTU15MSS. The comparison with Sentnal 3A tracks close to the coast of the Aleutian. illustrated some problems with the CLS15MSS.

The new DTU21MSS is computed over the same 20-year averaging time from 1993.01.01 to 2012.12.31 with a center time of 2003.01.01. Rio and Andersen (2007) derived a methodology to shift the center period of a MSS to consolidate data with a different averaging period e.g., C2 and S3A. However, we found that the 5year Sentinel-3A mean profiles (2016.05-2020.05) were too problematic to consolidate onto the 1993-2012 averaging period without degrading the MSS model, particularly in large current regions. This finally lead to the omission of these data in the DTU21MSS. We found that we need to extend the averaging period to 30 years soon to enable used the important new Sentinel-3A/B data in the next generation MSS models.

5 Author Contributions

OA wrote the manuscript and performed the computation of the DTU21MSS. ZS performed the two-pass retracking of all 20/40 Hz Geodetic Mission data. AA developing the software for producing 2 HZ and MSS computations in coastal regions. SKR performed the data processing for SAR and SARin data for the Polar Regions. SF contributed to the MSS validation in the Arctic Ocean.

6 Funding

ESA contributed to the MSS development through the BalticSeal project and the CryoTempo projects. SZ worked at DTU during 2020 supported by the National Nature Science Foundation of China, Grant No. 41804002, by the State Scholarship Fund of China Scholarship Council, Grant No. 201906085024, by Fundamental Research Funds for the Central Universities.

7 Acknowledgments

The authors are thankful to the space agencies for considering the Geodetic or Long-repeat missions as part of mission operations and for providing these high-quality data to the users. We would like to acknowledge ESA-RSS (Research and Service Support), and in particular B. Abis and G. Sabatino, the for their assistance in processing the data with G-POD (http://gpod.eo.esa.int/). We acknowledge the support of ESA to the CryoTempo and Baltic Seal+ project through the contracts AO/1-10244/20/I-NS & 4000126590/19/I-BG

8 Data availability statement

The DTU21MSS is available from http://data.dtu.dk. The high-resolution MSS model is available in several formats and relative to various reference ellipsoids (TOPEX and WGS84/GRS80) DOI: 10.11583/DTU.19383221

9 Reference

Andersen, O.B.; Zhang, S.; Sandwell, D.T.; Dibarboure, G.; Smith, W.H.F.; Abulaitijiang, A. (2021) The Unique Role of the Jason Geodetic Missions for High Resolution Gravity Field and Mean Sea Surface Modelling. *Remote Sens.*, *13*, 646. https://doi.org/10.3390/rs13040646

Andersen O.B, Knudsen P (1998) Global marine gravity field from the ERS-1 and Geosat geodetic mission altimetry. J Geophys Res 103:8129–8137

Andersen O. B, Knudsen P (2019) The DTU17 global marine grav- ity field: first validation results. In: International association of geodesy symposia, Berlin, Heidelberg. https://doi.org/10.1007/ 1345_2019_65

Andersen O. B, Scharroo R (2011) Range and geophysical corrections in coastal regions: and implications for mean sea surface determination. In: Vignudelli S, Kostianoy A, Cipollini P, Benveniste J (eds) Coastal altimetry. Springer, Berlin, pp 103–146

Andersen O. B, Knudsen P, Berry PAM (2010) The DNSC08GRA global marine gravity field from double retracked satellite altimetry. J Geod 84(3):191–199

Andersen O. B, Knudsen P, Kenyon S, Holmes S (2014) Global and Arctic marine gravity field from recent satellite altimetry (DTU13). In: Proceedings 76th EAGE conference and exhibition 2014, Amsterdam RAI, the Netherlands. http://doi.org/https://doi.org/ 10.3997/2214-4609.20140897

Brown, G., The average impulse response of a rough surface and its applications, IEEE Journal of oceanic engineering, 2(1), 67–74, 1977.

Dibarboure, G., Boy, F., Desjonqueres, J. D., Labroue, S., Lasne, Y., Picot, N., et al. (2014). Investigating short-wavelength correlated errors on low-resolution mode altimetry. Journal of Atmospheric and Oceanic Technology, 31, 1337–1362. https://doi.org/10.1175/JTECH-D-13-00081.1

Dinardo S., Fenoglio, L., Buchhaupt C., Becker M., Scharroo R., Fernandes M. J, Benveniste, J. (2018). Coastal SAR and PLRM altimetry in German Bight and West Baltic Sea. Advances in Space Research. 62. http://doi.org/10.1016/j.asr.2017.12.018

Dufau, C., Orstynowicz, M., Dibarboure, G., Morrow, R., & La Traon, P.-Y. (2016). Mesoscale resolution capability of altimetry: Present & future.

Journal of Geophysical Research, 121, 4910–4927. https://doi.org/10.1002/2015JC010904

Fu L-L, Cazenave A (2001) Satellite altimetry and earth sciences: a handbook of techniques and applications. Academic, San Diego

Garcia, E., S., Sandwell, D. T., Smith W.H.F. (2014) Retracking CryoSat-2, Envisat and Jason-1 radar altimetry waveforms for improved gravity field recovery, *Geophysical Journal International*, Volume 196, Issue 3, March 2014, Pages 1402–1422, https://doi.org/10.1093/gji/ggt469

Gommenginger, C. *et al.* (2011). Retracking Altimeter Waveforms Near the Coasts. In: Vignudelli, S., Kostianoy, A., Cipollini, P., Benveniste, J. (eds) Coastal Altimetry. Springer, Berlin, Heidelberg. https://doi.org/10.1007/978-3-642-12796-0_4

Helm, V., A. Humbert, H. Miller, (2014) Elevation and elevation change of Greenland and Antarctica derived from Cryosat-2, The Cryosphere, 8 (2014), pp. 1539-1559

Knudsen P, Brovelli M (1993) Collinear and cross-over adjustment of geosat erm and seasat altimeter data in the mediterranean sea. Surv Geophys 14(4–5):449–459

Lyard, F. H., Allain, D. J., Cancet, M., Carrère, L., and Picot, N.: FES2014 global ocean tide atlas: design and performance, Ocean Sci., 17, 615–649, https://doi.org/10.5194/os-17-615-2021, 2021

Maus, S., Green, C.M. and Fairhead, J.D., (1998) Improved ocean-geoid resolution from retracked ERS-1 satellite altimeter waveforms. Geophysical Journal International, 13 134(1), pp.243-253.

Pavlis NK, Holmes SA, Kenyon SC, Factor JK (2012) The development and evaluation of the earth gravitational model 2008 (EGM2008). J Geophys Res V117:B04406. https://doi.org/10.1029/2011J B008916

Pujol, M.-I., Schaeffer, P., Faugere, Y., Raynal, M., Dibarboure, G., and Picor, N. (2018) Gauging the improvement of recent mean sea surface models: A new approach for identifying and quantifying their errors, J. Geophys Res Oceans, 123, 5889-5911, Https://doi.org/10.1029/2017JC0013503

Raney, R. K., 2011. CryoSat-2 SAR mode looks revisited. *IEEE Geosci Remote Sensing Lett.*, **9**(3), pp.393–397.

Ray, C., C. Martin-Puig, M. P. Clarizia, G. Runi, S. Dinardo, C. Gommenginger, and J. Benveniste, SAR altimeter backscattered waveform model, IEEE Transactions on Geoscience and Remote Sensing, 53(2), 911–919, 2015.

Rio, M.-H., O. B. Andersen (2009) **GUT WP8100 Standards and recommended models, Report XXX, ESA**

Rose, S.K.; Andersen, O.B.; Passaro, M.; Ludwigsen, C.A.; Schwatke, C. Arctic Ocean Sea Level Record from the Complete Radar Altimetry Era: 1991–2018. *Remote Sens.* **2019**, *11*, 1672. https://doi.org/10.3390/rs11141672

Schaeffer, P., Faugere, Y., Legeais, J. F., Ollivier, A., Guinle, T., & Picot, N. (2012). The CNES CLS11 global mean sea surface computed from 16 years of satellite altimeter data. Marine Geodesy, 35, 3–19.

Scharroo, R., E. W. Leuliette, J. L. Lillibridge, D. Byrne, M. C. Naeije, and G. T. Mitchum (2013) , RADS: Consistent multi-mission products, in *Proc. of the Symposium on 20 Years of Progress in Radar Altimetry, Venice, 20-28 September 2012,* Eur. Space Agency Spec. Publ., ESA SP-710, p. 4 pp.

Sandwell, D.T. and Smith, W.H.F., 2005. Retracking ERS-1 altimeter waveforms for optimal gravity field recovery. Geophysical Journal International, 163(1), pp.79-89.

Sandwell D.T., Smith WHF (2009) Global marine gravity from retracked Geosat and ERS-1 altimetry: ridge segmentation versus spreading rate. J Geophys Res 114(B1): B01411

Sandwell D.T., Garcia ES, Soofi K, Wessel P, Chandler M, Smith W.H.F. (2013) Towards 1-mGal accuracy in global marine gravity from Cryosat-2, Envisat and Jason-1. Lead Edge 32:892–898

Sandwell D.T., Müller R.D., Smith W.H.F., et al (2014) New global marine gravity model from CryoSat-2 and Jason-1 reveals buried tectonic structure. Science 346(6205):65–67

Sandwell D.T., Harper H, Tozer B, Smith W.H.F. (2019) Gravity field recovery from geodetic altimeter missions. Adv Space Res. HTTPS:// doi.org/10.1016/j.asr.2019.09.011

Stammer D, Cazenave A (ed) (2017) Satellite altimetry over oceans and land surfaces. CRC Press, Boca Raton. https://doi.org/10.1201/ 9781315151779

Zhang S., Sandwell D.T. (2017) Retracking of SARAL/AltiKa radar altimetry waveforms for optimal gravity field recovery. Mar Geodesy 40(1):40–56

Zhang S, Sandwell D.T., Jin T, Li D (2017) Inversion of marine gravity anomalies over southeastern China seas from multi-satellite altimeter vertical deflections. J Appl Geophys 137:128–137

Zhang S, Li J, Jin T, Che D (2018) Assessment of radar altimetry cor- rection slopes for marine gravity recovery: a case study of Jason-1 GM data. J Appl Geophys 151:90–102

Zhang S, Andersen O.B., Kong X, Li H (2020) Inversion and validation of improved marine gravity field recovery in South China Sea by incorporating HY-2A altimeter waveform data. Remote Sens 12:802

Zlotniki, V., (1991) Sea Level differences across the Gulf Stream and Kuroshio extension. J. Physical Oceanog., 21(4), 599-609.

Rebecca A Woodgate, R. A, and Peralta-Ferriz, C. (2021) Warming and Freshening of the Pacific Inflow to the Arctic from 1990-2019 implying dramatic shoaling in Pacific Winter Water ventilation of the Arctic water column *Geophysical Research Letters, April 2021.DOI: 10.1029/2021GL092528*

WWW1, (2022) https://earth.esa.int/eogateway/news/cryosat-geographical-mode-mask-4-0-released